

## Anharmonic Keating model for group-IV semiconductors with application to the lattice dynamics in alloys of Si, Ge, and C

H. Rucker and M. Methfessel

*Institut für Halbleiterphysik, P.O. Box 409, D-15204 Frankfurt, Oder, Germany*

(Received 1 June 1995)

A generalization of the Keating model is given which treats anharmonic effects in a much improved manner. The dependence of the bond-stretching and bond-bending force constants on the crystal volume was determined by means of *ab initio* density-functional calculations, revealing simple universal scaling laws. The resulting anharmonic model was used to investigate optical phonons in disordered alloys of Si, Ge, and C. The calculated Raman spectra agree well with experimental results and are analyzed in terms of microscopic and macroscopic strain as well as confinement effects due to mass disorder.

### I. INTRODUCTION

In this paper, our aim is to derive a variant of the well-known Keating model<sup>1</sup> which is especially well suited to describe IV-IV substitutional semiconductor alloys, i.e., materials made from C, Si, Ge, and Sn. There is growing interest in such alloys, for example as a means to tailor the band gaps, band offsets, and the strain in pseudomorphic layer structures.<sup>2-5</sup> Interesting questions arise as to whether these alloys show ordering, what concentrations are attainable, and what the elastic properties and lattice dynamical properties of the alloy are.

To study these topics, one would like an accurate but reasonably efficient method to obtain the total energy of the crystal as a function of the atomic positions. In principle, a full *ab initio* treatment within density-functional theory (DFT) would be desirable because it includes all relevant effects without the need for adjustable parameters. However, the computational effort is large, leading to severe restrictions in the systems which can be handled in practice. For example, direct *ab initio* calculations are difficult for diluted alloys represented by large unit cells. Special approaches within the DFT framework are possible; for example, using perturbation theory with respect to the virtual crystal approximation, de Gironcoli *et al.*<sup>6</sup> were able to study the thermodynamics of  $\text{Si}_{1-x}\text{Ge}_x$  alloys. Unfortunately, a perturbative treatment seems to be much more complicated for C or Sn in Si and Ge because these elements cause strong perturbations of the lattice and of the electronic spectrum.

Alternatively, a much simpler and more efficient description based on the Keating model<sup>1</sup> (or similar approaches<sup>7,8</sup>) can be used. The energy of mixing relative to the pure materials is first separated into two parts:

$$E_{\text{mix}} = E_{\text{chem}} + E_{\text{strain}}, \quad (1)$$

where the chemical term  $E_{\text{chem}}$  arises because the strength of an  $AB$  bond might be different from the average of the  $AA$  and  $BB$  bond strengths and the strain

term  $E_{\text{strain}}$  derives from bond stretching and bending deformations. Both terms are essentially short ranged in covalent systems with small ionic character of the bonds. The strain contribution to the total energy is described by the Keating (or valence-force) model. This is a low-order expansion of the strain energy respective to atomic shifts relative to the perfect crystal lattice sites. The resulting energy expression is similar to that for point atoms connected by classical springs. The expansion coefficients (the force constants) are generally fitted to some external data such as the elastic constants or phonon frequencies. It is the strain contribution to the total energy which determines the local geometry, elastic properties, and lattice dynamics for an alloy with a given occupation of the lattice sites.

For the IV-IV alloys considered here, the standard Keating model is inadequate because of the strong local distortions which accompany alloying of Si and Ge with C or Sn. This can be seen from the drastically different equilibrium bond lengths, which are 1.55 Å for diamond-structure carbon, 2.35 Å for Si, 2.45 Å for Ge, and 2.81 Å for  $\alpha$ -Sn. The size differences are even more apparent when looking at the equilibrium volumes per atom, which are 5.7, 20.0, 22.5, and 34.0 Å<sup>3</sup> for C, Si, Ge, and Sn, respectively. This local volume is conserved to some extent in the alloy, making necessary perturbations of the bond lengths and angles which are much larger than those which are considered in the context of phonon frequencies and elastic properties.

Our purpose is to modify the Keating model to describe such strongly distorted systems properly. Clearly, the formalism must be extended to include higher-order anharmonic terms in some manner, but this can be done in many different ways. To avoid turning this topic into a simple matter of fitting more parameters to more data, we attempt a systematic approach as follows. First, we perform *ab initio* density-functional calculations to obtain reliable values of the elastic constants and selected phonon frequencies in the pure materials and the zincblende  $AB$  compounds. Hereby each lattice constant is varied over a range from compression to expansion which

is far beyond that which is accessible to experiment. The Keating force constants are fitted at each lattice constant  $a_i$  separately in the usual way. Next, we inspect the resulting functions  $\alpha(a)$  and  $\beta(a)$  and find that the dependence on  $a$  is given by simple scaling laws. To construct a model suitable for disordered systems, we postulate a suitable averaging procedure to define a bond-bending force constant for  $A$ - $A$ - $B$  type chains. The final model is tested against additional *ab initio* calculations.

The rest of this paper is organized as follows. The next section discusses the valence-force-field model and presents the anharmonic generalization as sketched above. The model has been applied previously to study the local atomic structure of  $\text{Si}_{1-x}\text{Ge}_x$  and  $\text{Si}_{1-x-y}\text{Ge}_x\text{C}_y$  alloys.<sup>9</sup> In Sec. III of the present paper we use it to investigate the vibrational spectra of  $\text{Si}_{1-x}\text{Ge}_x$ ,  $\text{Si}_{1-y}\text{C}_y$ , and  $\text{Si}_{1-x-y}\text{Ge}_x\text{C}_y$  alloys in comparison to experimental Raman results. A summary of the main results is given in Sec. IV.

## II. MODEL

This section has three parts. First, we briefly discuss the chemical contribution to the mixing energy; second, we collect the equations of the standard (harmonic) Keating model which are needed further on; third, we develop and test the anharmonic Keating model.

### A. Chemical contribution

The mixing energy (or enthalpy of formation) for a system containing  $m$  atoms of type  $A$  and  $n$  atoms of type  $B$  is<sup>10</sup>

$$E_{\text{mix}} = E[A_m B_n] - mE[A] - nE[B] \quad (2)$$

The ‘‘reservoir’’ energies  $E[A]$  and  $E[B]$  are the total energies per atom for the pure  $A$  and  $B$  crystals. The total energy of the mixed crystal  $E[A_m B_n]$  depends on the specific configuration in which the  $A$  and  $B$  atoms are arranged on the lattice. It is apparent that a chemical term is needed in the formalism because  $E_{\text{mix}}$  is nonzero for the ordered zinc-blende  $AB$  compounds, for which there can be no strain contribution. For these specific systems the chemical contribution equals the binding energy

$$E_{\text{chem}}[AB] = E_{\text{mix}} = E[AB] - E[A] - E[B] \quad (3)$$

This energy specifies whether the  $A$ - $B$  bond is stronger or weaker than the average of the  $A$ - $A$  and  $B$ - $B$  bond strengths. Table I presents these energies for all binary combinations of C, Si, Ge, and Sn in the cubic zinc-blende structure as calculated using the full-potential linear muffin-tin orbital (FP-LMTO) method (see below). Whereas the zinc-blende phase of SiC is stable ( $E_{\text{chem}} < 0$ ) with respect to separation into pure Si and diamond phases, all other possible zincblende phases are unstable ( $E_{\text{chem}} > 0$ ).

For the general case of an  $A_m B_n$  system, we make the

TABLE I. Calculated total energies per pair of atoms for possible zinc-blende structures of group-IV elements relative to the total energies of the diamond structures of the constituents [according to Eq. (3)]. All values are in eV.

	C	Si	Ge	Sn
C	0.0			
Si	-0.62	0.0		
Ge	0.74	0.044	0.0	
Sn	1.10	0.28	0.030	0.0

approximation that there is a chemical contribution to the  $A$ - $A$ ,  $B$ - $B$ , or  $A$ - $B$  bond strength which is invariant and transferable. Then the chemical contribution for the crystal can be assembled by counting the total number  $N_{AB}$  of  $A$ - $B$  bonds of the system:

$$E_{\text{chem}} = \frac{1}{4} N_{AB} E_{\text{chem}}[AB] \quad (4)$$

This is a relatively crude treatment; in truth, the chemical strength of a bond depends to some extent on the environment. For example, the Si-C bond at a carbon impurity in Si will not be exactly the same as in ordered silicon carbide because the participating silicon atoms are in different chemical environments. Possibly, a more accurate treatment of the chemical contribution is called for in some contexts, but we have not pursued this because the main interest here is on the strain energy.

### B. Harmonic Keating model

#### 1. Two-parameter model

It is well known that the elastic constants of diamond-structure crystals in equilibrium at the lattice constant  $a_0$  are well described by Keating’s two-parameter model.<sup>1</sup> The strain energy  $E_{\text{strain}}$  (denoted by  $W$  in the following for simplicity) is taken to depend on the vectors  $\mathbf{r}_{ij}$  which connect nearest-neighbor lattice sites  $i$  and  $j$  as follows:

$$W = \sum_{i,j} \frac{\alpha}{a_0^2} (\Delta(r_{ij}^2))^2 + \sum_{i,j,k \neq j} \frac{\beta}{a_0^2} (\Delta(\mathbf{r}_{ij} \cdot \mathbf{r}_{ik}))^2 \quad (5)$$

Here index  $i$  runs over all atoms and  $j$  and  $k$  run over the four nearest neighbors of atom  $i$ . In this expression,  $\Delta$  denotes the change relative to the perfect lattice due to a distortion, i.e.,  $\Delta(\mathbf{r}_{ij} \cdot \mathbf{r}_{ik}) = \mathbf{r}_{ij} \cdot \mathbf{r}_{ik} - \mathbf{r}_{ij}^0 \cdot \mathbf{r}_{ik}^0$  is the change in the scalar product between the two vectors connecting atom  $i$  with its neighbors  $j$  and  $k$ . Both  $\alpha$  and  $\beta$  have the dimension of a force constant (energy divided by length squared) because of the factors  $1/a_0^2$  in the definition. The atomic indices of the force constants  $\alpha$  and  $\beta$  were suppressed in Eq. (5).

The constants  $\alpha$  and  $\beta$  essentially describe the bond-stretching and bond-bending restoring forces (although bond-length distortions also enter via the second term since they change the scalar product even at a fixed bond angle). Parameters  $\alpha$  and  $\beta$  are usually fitted

to reproduce the elastic constants and phonon frequencies to those obtained experimentally or from *ab initio* calculations. Equation (5) leads to simple expressions for the bulk modulus, the two independent elastic shear constants, and the zone-center optical phonon frequency  $\omega_0 = \omega_{\text{TO}}(\Gamma)$  of a diamond-structure crystal:

$$B = \frac{1}{3}(C_{11} + 2C_{12}) = \frac{1}{a_0} \left( \alpha + \frac{1}{3}\beta \right), \quad (6)$$

$$C_{11} - C_{12} = \frac{4}{a_0} \beta, \quad (7)$$

$$C_{44} = \frac{4}{a_0} \frac{\alpha\beta}{\alpha + \beta}, \quad (8)$$

$$m\omega_0^2 = 8(\alpha + \beta), \quad (9)$$

where  $m$  is the reduced atomic mass. The two-parameter Keating model also implies that the three elastic constants are related by<sup>1</sup>

$$\frac{2C_{44}(C_{11} + C_{12})}{(C_{11} - C_{12})(C_{11} + 3C_{12})} = 1. \quad (10)$$

This condition is well satisfied for the diamond-structure semiconductors. Using the measured elastic constants, the left hand side of Eq. (10) gives 1.00, 1.01, and 1.07, for diamond, Si, and Ge, respectively. This confirms that all three elastic constants can be well described although only two fitting parameters are available.

Note that the bonds between two group-IV elements can have a significant polarity. The effective force constants  $\alpha$  and  $\beta$  account only for the short-range part of the electrostatic forces whereas the long-range electrostatic forces which arise for polarized bonds are neglected in the Keating model. In general the effect of long-range interactions on the strain energy of group-IV compounds is expected to be small, but these forces can become important for an exact description of the phonon dispersion. For instance, they cause the splitting of the longitudinal and transversal optical phonon frequencies at  $\Gamma$  in  $\beta$ -SiC.

## 2. Improvement of the two-parameter model for diamond

For the rest of this subsection, we digress to the topic of improving the two-parameter Keating model by adding additional force constants. The main features of the experimental phonon spectrum are reproduced within the simple Keating model fitted to the elastic constants, but there are considerable deviations in certain regions of the Brillouin zone. The major deviations are (i) the zone-center optical phonon frequency  $\omega_0$  is overestimated by 17%, 6%, and 1% for C, Si, and Ge, respectively (this means the phonon force constant is too large by 37% in diamond); and (ii) the Keating model gives a poor

description of the flattening of the transversal acoustic phonon branch near the zone boundary for Si, Ge, and  $\alpha$ -Sn.

It has been shown that inclusion of further interaction terms can improve the calculated dispersion. The phonon frequencies of all four diamondlike crystals could be satisfactorily described by a six-parameter model.<sup>8</sup> For Si and Ge the number of independent parameters could be reduced to four with almost the same accuracy.<sup>11</sup> We point out here that this model, although optimal for studying Si and Ge systems, cannot repair the discrepancy in  $\omega_0$  in carbon. Instead, one of the discarded interactions must be reincluded.

The Keating model includes two of the leading terms in a systematic expansion of the strain energy in terms of valence forces, namely the nearest-neighbor (NN) two-body force  $\alpha$  and one three-body force  $\beta$ . The general valence-force-field model has one NN two-body force ( $\alpha$ ) and three distinct NN three-body forces ( $\beta, \gamma, \kappa$ ), shown schematically in Fig. 1(b). Of these only the angular force term  $\beta$  is included in the Keating strain energy [Eq. (5)]. The two neglected three-body terms describe the correlation of the angle distortion with the length change of one leg,

$$W_\gamma = \sum_{i,j,k \neq j} \frac{\gamma}{a_0^2} \Delta(r_{ij}^2) \Delta(\mathbf{r}_{ij} \mathbf{r}_{ik}), \quad (11)$$

and the correlation between the length changes of two neighboring bonds,

$$W_\tau = \sum_{i,j,k \neq j} \frac{\tau}{a_0^2} \Delta(r_{ij}^2) \Delta(r_{ik}^2). \quad (12)$$

In an investigation of the role of the different three-body forces in Si and Ge, Sui and Herman<sup>11</sup> found that the length-length correlation  $\tau$  is important for an ac-

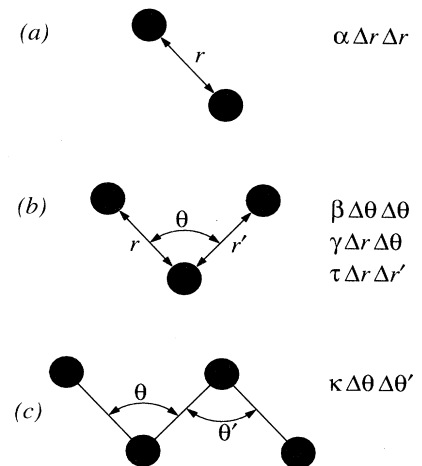


FIG. 1. Schematic representation of nearest-neighbor forces: (a) the two-body force, (b) the three-body forces, (c) a specific four-body force.

curate overall representation of the the phonon dispersion curves. Furthermore, it has been determined that a four-body force  $\kappa$  [Fig. 1(c)] is needed to describe the zone-boundary softening of the transverse acoustical branch,<sup>8,11</sup> whereas the length-angle correlation  $\gamma$  can be neglected. Trying to fit diamond using these parameters, we have found that the discrepancy in  $\omega_0$  cannot be removed. On the other hand, we have seen that all four quantities  $C_{11}$ ,  $C_{12}$ ,  $C_{44}$ , and  $\omega_0$  can be described simultaneously to good precision using the three force constants  $\alpha$ ,  $\beta$ , and  $\gamma$ . Since the zone-boundary softening is small for diamond, this gives a model with good overall agreement.

To see this, consider the expressions for the elastic constants and the zone-center optical phonon within this “ $\alpha$ ,  $\beta$ ,  $\gamma$ ” model:

$$B = \frac{1}{a_0} \left( \alpha + \frac{1}{3}\beta - \gamma \right), \quad (13)$$

$$C_{11} - C_{12} = \frac{4\beta}{a_0}, \quad (14)$$

$$C_{44} = \frac{4\alpha\beta - \gamma^2}{a_0(\alpha + \beta + \gamma)}, \quad (15)$$

$$m\omega_0^2 = 8(\alpha + \beta + \gamma). \quad (16)$$

In analogy to Keating’s relation (10) for the three elastic constants, one obtains a relation between  $C_{11}$ ,  $C_{12}$ ,  $C_{44}$ , and  $\omega_0$ :

$$\frac{4\eta C_{44}}{2(C_{11} - C_{12})(C_{12} + \eta) - [\eta - \frac{1}{2}(C_{11} + C_{12})]^2} = 1, \quad (17)$$

where  $\eta = m\omega_0^2/8a_0$ . For diamond, Si, and Ge the left-hand side evaluates to 0.97, 0.97, and 1.06, respectively, using the experimental data. This shows that all four quantities can be reproduced simultaneously even though only three parameters are available.

Based on these results, a relatively clear picture of the different three-body force terms results. The length-length correlation  $\tau$  accounts for the tendency to strengthen neighboring bonds when one bond is stretched. The length-angle correlation  $\gamma$  describes the tendency to reduce the bond length when the bond angles are increased from perfect tetrahedral bonding ( $sp^3$ ) towards planar bonding ( $sp^2$ ). Whereas the force constant  $\tau$  was shown to be important for an overall improvement of the fit to the Si and Ge phonon dispersion curves,<sup>11</sup> the force constant  $\gamma$  is needed for a simultaneous fit of the elastic constants and the zone center optical phonon in diamond. The four-body force  $\kappa$  can account for the reduced stability of the tetrahedral network with increasing metallicity of the atoms, an effect which can alternatively be described by the adiabatic motion of bond charges.<sup>12</sup>

Thus, by including additional force constants we can overcome most of the shortcomings of the two-parameter Keating model. However, in the present study the in-

teratomic force constants within the standard two-parameter Keating model. Hereby  $\alpha$  and  $\beta$  were determined from a least-squares fit to the elastic constants  $B$  and  $C_{11} - C_{12}$  and the squared phonon frequencies  $\omega_0$ . For the difficult case of diamond (see the preceding section) this gives  $B = 376$  GPa,  $C_{11} - C_{12} = 891$  GPa, and  $\omega_0 = 43.4$  THz. These values deviate up to 15% from the experimental values (442 GPa, 951 GPa, and 39.9 THz,

the distortion of the local bonding geometry can be very large in alloys such as  $\text{Si}_{1-x}\text{C}_x$  and  $\text{Ge}_{1-x}\text{Sn}_x$  in which the constituents have strongly different sizes. Such large distortions cannot be realized experimentally by applying external strain to the pure components and zincblende compounds. The advantage of *ab initio* calculations is that reliable results can be obtained for any possible strain including large negative pressures.

The full-potential linear muffin-tin orbital method<sup>13</sup> (FP-LMTO) was used for all *ab initio* calculations. Technical details are similar to those in previous calculations for diamond and Si,<sup>14</sup>  $\beta$ -SiC,<sup>15</sup> and  $\alpha$ -Sn.<sup>16</sup> The equal-sized almost touching muffin-tin spheres (including two empty spheres per unit cell) were scaled with the lattice constant. The LMTO basis consisted of tripled  $s$ ,  $p$ , and doubled  $d$  functions on the atoms with none placed on the empty spheres. The charge density was expanded in spherical Hankel functions up to  $\ell_{\text{max}} = 6$ . The Ceperly-Alder form for the LDA exchange-correlation potential was used. All calculations were nonrelativistic except for those cases which involved Sn, which were treated in the scalar-relativistic approximation. As discussed in Ref. 16, the results for  $\alpha$ -Sn depend to some extent on the way in which the corelike Sn  $4d$  states are treated. Here, these were treated as semicore states in a second energy panel. The same was done for the Ge  $3d$  states.

Calculations were done to obtain the the lattice parameters, the elastic constants, and the zone-center optical phonon frequencies for the diamond phases of C, Si, Ge, and Sn and for the zinc-blende compounds of these elements. The results for the diamond phases and for  $\beta$ -SiC are summarized in Table II together with experimental values. There is a very good agreement between experiment and theory for all the considered quantities. Calculated elastic constants  $B$  and  $C_{11} - C_{12}$  and phonon frequencies  $\omega_0$  for other hypothetical zinc-blende structures of group-IV elements are given in Table III.

The calculated properties were used to fit the interatomic force constants within the standard two-parameter Keating model. Hereby  $\alpha$  and  $\beta$  were determined from a least-squares fit to the elastic constants  $B$  and  $C_{11} - C_{12}$  and the squared phonon frequencies  $\omega_0$ . For the difficult case of diamond (see the preceding section) this gives  $B = 376$  GPa,  $C_{11} - C_{12} = 891$  GPa, and  $\omega_0 = 43.4$  THz. These values deviate up to 15% from the experimental values (442 GPa, 951 GPa, and 39.9 THz,

TABLE II. Calculated lattice constant, elastic constants, and zone-center optical phonon frequencies for C, Si, Ge,  $\alpha$ -Sn, and  $\beta$ -SiC. Experimental values are given in parentheses.

	C	Si	Ge	Sn	SiC
$a$ (Bohr)	6.68 (6.75) <sup>a</sup>	10.21 (10.26) <sup>a</sup>	10.66 (10.68) <sup>a</sup>	12.27 (12.26) <sup>a</sup>	8.17 (8.24) <sup>a</sup>
$B$ (GPa)	467 (442) <sup>a</sup>	96 (98) <sup>a</sup>	74 (76) <sup>a</sup>	43 (43) <sup>c</sup>	229 (225) <sup>b</sup>
$C_{11} - C_{12}$ (GPa)	955 (951) <sup>a</sup>	101 (102) <sup>a</sup>	83 (82) <sup>a</sup>	38 (40) <sup>c</sup>	267 (248) <sup>b</sup>
$C_{44}$ (GPa)	581 (577) <sup>a</sup>	81 (80) <sup>a</sup>	70 (68) <sup>a</sup>	37 (36) <sup>c</sup>	256 (256) <sup>b</sup>
$\omega_{\text{TO}}(\Gamma)$ (THz)	39.8 (39.9) <sup>a</sup>	15.6 (15.5) <sup>a</sup>	9.1 (9.1) <sup>a</sup>	5.9 (6.0) <sup>c</sup>	24.3 (23.9) <sup>b</sup>

<sup>a</sup>Landolt-Börnstein (Ref. 17).

<sup>b</sup>For a discussion of experimental values, see Ref. 15.

<sup>c</sup>Reference 18.

respectively). The obtained force constants and the calculated equilibrium bond length are given in Table IV. This two-parameter model is the starting point for the anharmonic generalization described next.

## 2. Scaling laws for the force constants

The Keating potential as introduced in Eq. (5) was designed to describe correctly the lowest-order contribution to the strain energy, i.e., terms which are quadratic in the distortion of the equilibrium geometry. Since the bonding curve of a crystal deviates considerably from the quadratic form for large distortions of the crystal volume, it is obvious that higher-order terms in the strain energy must be included for a reasonable description of large deformations of the atomic structure. One way to include higher-order terms is to use force constants which depend explicitly on the local geometry. Within the local picture of a valence-force model the two-body force constant

$$\alpha_{ij} = \alpha_{ij}^0 f(r_{ij}) \quad (18)$$

should depend on the interatomic distance  $r_{ij}$  only whereas the three-body force constant

$$\beta_{ijk} = \beta_{ijk}^0 g(r_{ij}, r_{ik}, \theta_{ijk}) \quad (19)$$

depends in general on the two involved bond lengths and

TABLE III. Results of *ab initio* calculations for the elastic constants  $B$  and  $C_{11} - C_{12}$  and phonon frequency  $\omega_{\text{TO}}(\Gamma)$  of hypothetical zinc-blende structures. The data were used to fit the force constants given in Table IV.

	$B$ (GPa)	$C_{11} - C_{12}$ (GPa)	$\omega_{\text{TO}}(\Gamma)$ (THz)
GeC	188	222	21.2
GeSi	85	95	12.6
SnC	133	122	19.9
SnSi	63	61	10.9
SnGe	56	53	7.5

on the enclosed angle  $\theta$ .

In order to study the bond length dependence of the force constants we have calculated the elastic constants for a large range of lattice constants, i.e., for extremely large positive and negative hydrostatic strain. In the following we discuss the results for Si. The same calculations carried out for diamond, Ge, and  $\beta$ -SiC then confirmed the conclusions concerning the scaling behavior of the force constants.

We start with the discussion of the bond-bending parameter  $\beta$ . Equation (7) shows that  $\beta$  is closely related to the elastic constant  $C_{11} - C_{12}$  which is associated with the strain  $\mathbf{e} = (e_1, e_2, e_3, e_4, e_5, e_6) = (\xi/2, \xi/2, -\xi, 0, 0, 0)$ . At the equilibrium volume, various other distortions can be used to obtain the same energy change to second order, for example one which strictly conserves the volume to all orders. Away from the equilibrium volume these distortions lead to different results (see the next subsection). To isolate the dependence of  $\beta$  it is more convenient to use a distortion which strictly maintains the bond lengths, given by  $e_1 = e_2 = \sqrt{1 + \xi} - 1$ ,

TABLE IV. Keating parameters  $\alpha$  and  $\beta$  as determined from a least square fit to the calculated elastic constants and zone center optical phonons and equilibrium lattice constants of the corresponding diamond and zinc-blende structures. Force constants and lattice constants are given in atomic units.

	$a_0$	$\alpha$	$\beta$
C	6.68	0.137	0.101
Si	10.21	0.058	0.017
Ge	10.66	0.049	0.015
Sn	12.27	0.034	0.008
SiC	8.17	0.088	0.036
GeC	8.54	0.081	0.031
GeSi	10.43	0.053	0.017
SnC	9.14	0.074	0.019
SnSi	11.25	0.045	0.012
SnGe	11.44	0.041	0.010

$e_3 = \sqrt{1-2\xi} - 1$ ,  $e_4 = e_5 = e_6 = 0$ . Substituting this distortion into the Keating energy [Eq. (5)] and differentiating gives

$$\frac{2}{3V} \frac{d^2W}{d\xi^2} = \frac{4a}{a_0^2} \beta(a) =: G(a) \quad (20)$$

Thus the scaling of the force constant  $\beta$  can be obtained directly from the scaling of  $G$ . From *ab initio* calculations for different crystal volumes  $V$  we have found that  $G(V)$  is proportional to the inverse of the square of the crystal volume. Consequently  $G$  depends on the lattice parameter  $a$  via the power law

$$G(a) = \left(\frac{a_0}{a}\right)^6 G(a_0) \quad (21)$$

and  $\beta(a)$  scales as  $a^{-7}$ . According to Eq. (19), the bond-bending force constant  $\beta_{ijk}$  is assumed to be a function of the lengths  $r_{ij}$  and  $r_{ik}$  of the two involved bonds. For inhomogeneous distortions the two bonds will generally be stretched differently. Generalizing the scaling to this case we assume

$$\beta_{ijk} = \beta_{ijk}^0 \left(\frac{r_{ij}^0}{r_{ij}}\right)^{7/2} \left(\frac{r_{ik}^0}{r_{ik}}\right)^{7/2}, \quad (22)$$

where  $r_{ij}$  and  $r_{ij}^0$  are the strained and unstrained bond lengths, respectively. Although other ways to average could also be used, this choice seems most natural because it is compatible with the derived scaling law. Note also that for a heteropolar crystal such as SiC, the calculation of  $G$  can only give the average of the bond-bending force constants  $\beta_{\text{Si-C-Si}}$  and  $\beta_{\text{C-Si-C}}$ . Due to lack of additional information we have taken the two constants to be equal.

Next, we use the bonding curves as obtained from the *ab initio* calculations to determine the bond-length dependence of the bond-stretching force constant  $\alpha$ . Calculated total energies for a wide range of crystal volumes are shown in Fig. 2 relative to the total energy  $E_{\text{tot}}(V_0)$  at the equilibrium volume  $V_0$ . In the Keating model the bonding curve is mainly determined by the bond-stretching force constant  $\alpha$  and to a smaller extent by

the bond-bending force constant  $\beta$ . Assuming a power law

$$\alpha_{ij} = \alpha_{ij}^0 \left(\frac{r_{ij}^0}{r_{ij}}\right)^n \quad (23)$$

and using the previously determined scaling for  $\beta$ , we find very good agreement with the DFT results for  $n = 4$ . Results of the Keating model with force constants scaled according to Eqs. (22) and (23) are shown as a solid line in Fig. 2. The model reproduces DFT results far beyond the harmonic range. It should be mentioned that the exponent  $n = 4$  in Eq. (23) guarantees that the energy goes to a constant value for large lattice constants, i.e., in the limit of free atoms. However, this limit is not expected to reproduce the correct binding energy of the crystal since the spin-polarization of the free atoms and the dehybridization of the  $sp^3$  orbitals are not included in Keating's model.

As a first test of the obtained scaling laws for the force constants, we have calculated the zone-center optical phonon frequencies  $\omega_0$  for different crystal volumes  $V$  using *ab initio* DFT and the Keating model with the scaled force constants. We find comparably good agreement as for the bonding curve (Fig. 3). Also, the mode Grüneisen parameter  $\gamma = -d \ln \omega_0 / d \ln V$  is well reproduced as can be seen from the values given in Table V, showing that  $\omega_0$  scales as the reciprocal volume.<sup>19</sup> Note that the standard Keating model obtains the mode Grüneisen parameter with the wrong sign.

Up to now we have not specified any dependence of the force constant  $\beta$  on the bond angle  $\theta$ . For the considered cases including lattice deformations with large-angle distortions the *ab initio* results could be well reproduced when the force constants depend on the bond length only. However, the model in this form does not give correct values for the uniaxial deformation potential of zone-center optical phonons under a (001) distortion. In order to fit this quantity [denoted<sup>19</sup> by  $(p-q)/2\omega_0^2$ ] we must include the angular dependence of  $\beta$ . Assuming a power law

$$\beta_{ijk} = \beta_{ijk}^0 \left(\frac{r_{ij}^0}{r_{ij}}\right)^{7/2} \left(\frac{r_{ik}^0}{r_{ik}}\right)^{7/2} \left(\frac{\theta_0}{\theta}\right)^\nu \quad (24)$$

we have fitted the exponent  $\nu$  for Si and Ge to repro-

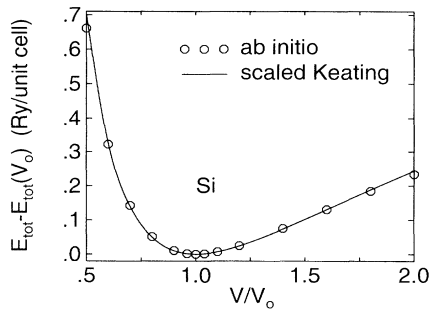


FIG. 2. Energy-volume curve for Si determined from *ab initio* DFT calculations (circles) and from the anharmonic Keating model using the universal scaling parameters (line).

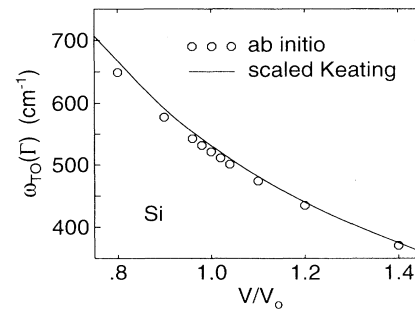


FIG. 3. Volume dependence of the zone-center optical phonon frequency in Si as determined from *ab initio* DFT calculations (circles) and from the anharmonic Keating model (line).

duce the measured uniaxial phonon deformation potentials given in Table V. The results of *ab initio* DFT calculations for the uniaxial phonon deformation potentials are close to the experimental values.<sup>13</sup> However, the obtained exponent  $\nu$  depends strongly on the values of the force constants  $\alpha$  and  $\beta$ . These can be different depending on whether more emphasis is put on the elastic constants or the phonon frequencies in the fit. No universal scaling law was found for the angular dependence of the bond-bending force constant  $\beta$ .

The final anharmonic Keating model is given by the usual expression [Eq. (5)], but with the constants  $\alpha$  and  $\beta$  substituted by the simple functions of the bond lengths (and possibly the bond angle) which were derived in this section. For a given set of Keating parameters the harmonic and anharmonic models agree to second order in the atomic displacements, as can be seen from Eq. (5). Thus both models give the same results for the equilibrium geometry, the phonon dispersion, and the elastic constants. Any inadequacies in the harmonic model for these quantities (say, a wrong description of the soft zone-boundary TA phonon modes) are not fixed by putting in the scaling of the force constants. Instead, the gain is a more correct description of quantities which are sensitive to anharmonic terms. The simplest example is the substantial improvement in the mode Grüneisen parameters mentioned above. Another such property is the change in an elastic constant with the volume, considered next.

### 3. Test of the model

The anharmonic Keating model introduced above was based on *ab initio* calculations for selected long-wave distortions in bulk crystal under extreme conditions. In the following we (i) check the results obtained for the full set of elastic constants and (ii) test the model against additional *ab initio* calculations for inhomogeneous systems with large local strain fields.

To check the elastic constants, it is useful to have an expression for the strain energy for a given distortion when the crystal is not at its equilibrium volume. The

TABLE V. Mode Grüneisen parameters and uniaxial phonon deformation potentials  $(p - q)/2\omega_0^2$  for (001) distortions for Si and Ge. Results of LDA calculations are compared with experimental values and with results from the scaled Keating model. The exponents  $\nu$  were fitted to reproduce the experimental uniaxial deformation potentials.

	Si	Ge
$\gamma$ (LDA)	0.98	0.99
$\gamma$ (exp)	0.98 <sup>a</sup>	0.96 <sup>a</sup>
$\gamma$ (Keating)	1.03	1.02
$(p - q)/2\omega_0^2$ (exp)	0.23 <sup>b</sup>	0.23 <sup>c</sup>
$\nu$	0.93	1.0

<sup>a</sup>Reference 20.

<sup>b</sup>Reference 21.

<sup>c</sup>Reference 19.

expansion of the energy per volume  $w = W/V$  to second order in the strain  $\mathbf{e} = (e_1, \dots, e_6)$  has a linear as well as a quadratic term:

$$w = \frac{1}{2} \mathbf{e}^T C \mathbf{e} - p(V)(e_1 + e_2 + e_3), \quad (25)$$

where  $C$  is the usual  $6 \times 6$  matrix of elastic stiffness constants (with independent components  $C_{11}$ ,  $C_{12}$ , and  $C_{44}$  for a cubic system). The coefficient of the linear term  $-p(V) = V \partial w / \partial V$  is the negative of the external pressure needed to keep the crystal at the volume  $V$ , as follows from cubic symmetry and by considering a homogeneous volume change. A “special-purpose” distortion (for example, one which strictly maintains the volume or the bond lengths) is described by strains which are functions of some parameter  $\xi$ ,

$$e_\nu = f_\nu(\xi) = a_\nu \xi + b_\nu \xi^2 + \dots$$

The quadratic terms  $b_\nu \xi^2$  modify the quadratic term in the energy, as follows by substituting  $e_\nu$  in Eq. (25):

$$w = \left( \frac{1}{2} \mathbf{a}^T C \mathbf{a} + V \frac{\partial w}{\partial V} (b_1 + b_2 + b_3) \right) \xi^2 - p(V)(a_1 + a_2 + a_3) \xi, \quad (26)$$

where  $\mathbf{a} = (a_1, \dots, a_6)$ . For the bond-length conserving tetragonal distortion used above this evaluates to

$$w = \left[ \frac{3}{4} (C_{11} - C_{12}) + \frac{3}{4} p(V) \right] \xi^2. \quad (27)$$

The first term in the brackets is the result when the strain is simply  $\mathbf{e} = (-\xi/2, -\xi/2, \xi, 0, 0, 0)$ . Alternatively, for the strictly volume-conserving tetragonal distortion  $e_1 = e_2 = \xi/2$ ,  $e_3 = (1 + \xi/2)^{-2} - 1$  we obtain the same expression but with a negative sign of the pressure term. Similarly, the volume-conserving trigonal distortion is  $e_1 = e_2 = e_3 = (1 + 3\xi/2)^{-1/3} + \xi/2 - 1$ ,  $e_4 = e_5 = e_6 = \xi$  and the energy change is

$$w = \left[ \frac{3}{2} C_{44} - \frac{3}{2} p(V) \right] \xi^2. \quad (28)$$

Figure 4 compares for the case of silicon elastic constants and the pressure obtained with the anharmonic Keating model with the *ab initio* results as a function of the volume. There is very good agreement over the whole range of considered volumes, showing the validity of the scaling laws for  $\alpha$  and  $\beta$ . For comparison, in a harmonic model the pressure goes linear with the crystal volume and the elastic constants are almost independent on volume. Note that whereas a scaling of  $V^{-2}$  was found for the energy change for a tetragonal distortion at constant bond length [the quantity  $G(V)$  introduced above], the related elastic constant  $C_{11} - C_{12}$  behaves quite differently. To a reasonable degree, we find that  $C_{11} - C_{12}$  and  $C_{44}$  scale as approximately  $V^{-1}$  and  $V^{-2}$ , respectively. These scaling laws are different from an estimate using Harrison’s tight-binding model which gave an  $a^{-5}$  scaling for  $C_{11} - C_{12}$  based on a comparison of different materials at their equilibrium lattice constants.<sup>22,23</sup>

As a test case for inhomogeneous systems, we consider three arrangements of substitutional carbon atoms in a

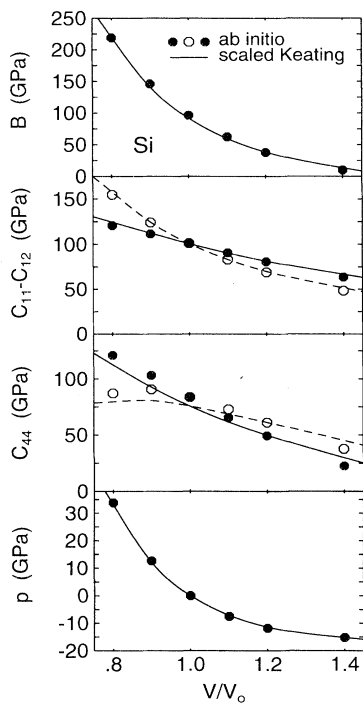


FIG. 4. Comparison of the elastic constants and the pressure as a function of the volume as determined using the *ab initio* calculation (circles) and the anharmonic Keating model (line). These were obtained by calculating the quantities shown as dashed lines and as open circles and applying the transformations given in the text. The quantity calculated directly was the stiffness for a distortion which conserves the bond lengths (for  $C_{11} - C_{12}$ ) and the volume (for  $C_{44}$ ).

Si lattice. Local deformations are very large in this case because of the short Si-C bond. Details of the *ab initio* FP-LMTO calculations were as described in Ref. 24.

First, a single C atom in a Si lattice is considered, represented here by a supercell of 32 atoms. The energy per C atom is shown in Fig. 5(a) when the nearest-neighbor Si atoms are displaced towards the C atom. All other atoms stay at the ideal lattice positions. The geometry parameter  $\xi$  describes the relaxation of the Si-C bond length  $d_{\text{SiC}} = d_{\text{Si}}(1 - \xi)$ , where  $d_{\text{Si}}$  is the bond length in a Si crystal. Second, we consider a hypothetical (001) monolayer of C atoms in a Si lattice [Fig. 5(b)]. The spacing  $h = a_{\text{Si}}(\frac{1}{4} - \xi)$  between the C layer and the neighboring Si layers is varied as described by the parameter  $\xi$ . Third, half a monolayer of a C atom is arranged on a (001) plane in a  $(\sqrt{2} \times \sqrt{2})$  unit cell. Energies for different spacings between the C-containing layer and the neighboring Si layers are given in Fig. 5(c). The energy was minimized respective to the  $x$  and  $y$  coordinates of the Si atoms in the adjacent layers. All energies of formation given in Figs. 5(a)–5(c) are differences between the total energy of the supercell (containing one carbon atom) relative to the pure Si and  $\beta$ -SiC crystals.

For comparison, the figure also shows the energies obtained using the standard Keating model for the same

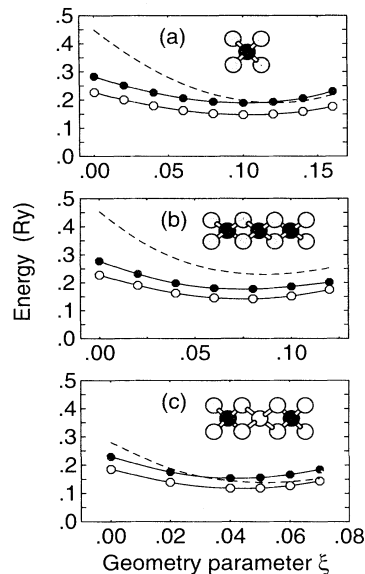


FIG. 5. Energy of formation for different arrangements of substitutional C atoms in a Si lattice: (a) single substitutional C impurity in a 32-atom supercell, (b) (001) monolayer of C atoms in a Si lattice, (c) half monolayer of a C atom arranged on a (001) plain in a  $(\sqrt{2} \times \sqrt{2})$  unit cell. The relaxation of the local geometry is always expressed by a single parameter  $\xi$  as specified in the main text. Insets indicate the nearest-neighbor environments of the C atoms (black) for the three cases. Results of *ab initio* calculations (full symbols) are differences between the total energy of the supercell and the total energies of the constituent atoms in the Si and  $\beta$ -SiC phases. All supercells contain one carbon atom. Open symbols are results of the anharmonic Keating model. Lines are indicated to guide the eye.

force constants. The anharmonic terms lead to large improvement in the calculated energy surface. The positions of the minima and the curvatures are well reproduced, showing that relaxed geometries and phonon frequencies are reliable. However, the absolute values of the energies obtained from the anharmonic Keating model are systematically about 50 mRy too low. This discrepancy is mainly due to the limitations of the two-parameter Keating model. Similar to the case of diamond discussed in Sec. IIB 2, the elastic constants and zone-center optical phonon of  $\beta$ -SiC cannot be reproduced simultaneously using only  $\alpha$  and  $\beta$  as fit parameters. Consequently the force constants determined from a fit to the elastic constants and the zone-center optical phonon (see Table IV) lead to a bulk modulus which is about 20% too small. This Keating model underestimates the energy cost for stretching the Si-C bonds when the C atom is incorporated into the Si lattice. The difference between the energies obtained from DFT and from the Keating model are not due to chemical contributions. Chemical contributions to the formation energy could arise from differences between the bonding of substitutional C in Si and the bonding in  $\beta$ -SiC. However, these terms are



small as is evident from the fact that the energy for the ideal unrelaxed positions can be well estimated from the work needed to strain SiC to the Si lattice constant.

### III. OPTICAL PHONONS IN STRAINED $\text{Si}_{1-x}\text{Ge}_x\text{C}_y$ LAYERS

The preceding section has presented the anharmonic Keating model and has shown that the energy of *ab-initio* calculations can be modeled accurately even for the extreme case of mixtures of Si and C. This gives us the confidence to use the model to study the phonon frequencies in disordered alloys containing Si, Ge, and C. When Ge atoms are added to a Si crystal, the Si-Si phonon modes shift to lower frequencies. A starting point is to attribute this to a softening of the Si-Si bonds as they adapt to the larger average lattice constant in the alloy. Interestingly, however, a similar softening is seen for the Ge-Ge modes when Si atoms are added to a Ge crystal, even though the Ge bonds become *shorter* in the alloy. Menendez *et al.*<sup>26</sup> could explain the measured shifts qualitatively as a competition between confinement and strain effects. The aim of our calculations is to confirm this explanation and to quantify the different contributions.

#### A. Calculation of Raman spectra

The optical phonon spectra of alloys of group-IV elements are characterized by individual branches in the vibration spectrum which correspond to the different types of nearest-neighbor bonds in the alloy. Thus the Raman spectrum of a  $\text{Si}_{1-x}\text{Ge}_x$  alloy reveals three main branches corresponding to Si-Si, Si-Ge, and Ge-Ge modes. In a dilute  $\text{Si}_{1-y}\text{C}_y$  alloy, Si-Si, and Si-C phonons can be identified; while C-C modes are in principle possible, they are not observed due to the low probability of C-C nearest-neighbor pairs. The phonon spectrum of an *AB* alloy with large differences in the atomic masses cannot be described by any model which does not explicitly consider *AA*, *AB*, and *AB* nearest-neighbor pairs. For  $\text{Si}_{1-x}\text{Ge}_x$  alloys it was demonstrated by de Gironcoli and Baroni<sup>25</sup> that the coherent potential approximation (CPA) cannot account for the three-mode behavior of the optical phonons. Consequently, a more appropriate theoretical description of the phonon spectra is based on the actual microscopic arrangement in a supercell with several hundred randomly distributed atoms.

To simulate the random alloy, we use 512-atom supercells with the atoms distributed at random over the lattice sites according to the stoichiometry. For a given configuration the atomic positions are relaxed using the anharmonic Keating model until the forces vanish. The resulting microscopic geometry, especially the distribution of nearest-neighbor bond lengths as a function of the stoichiometry, has been discussed previously.<sup>9</sup> For the relaxed atomic positions we directly calculate the full dynamical matrix as the second derivative of the Keating energy. Phonon frequencies and eigenvectors are ob-

tained from the diagonalization of the dynamical matrix. Raman selection rules are incorporated as in Ref. 30. Assuming the same polarizability for all atoms, the off-resonance Raman intensity is given, up to a multiplicative constant, by

$$\sigma^{xy} \propto \sum_{\nu} \frac{\delta(\omega_{\nu} - \omega)}{\omega_{\nu}} \left| \sum_i s_i u_{iz}^{\nu} \right|^2, \quad (29)$$

where  $\nu$  runs over all phonon modes,  $u_{iz}^{\nu}$  is the  $z$  component of the displacement of the atom at lattice site  $i$ , and  $s_i$  is +1 and -1 for the two fcc sublattices of the diamond structure. The final Raman spectra are obtained by averaging over typically 10 to 15 configurations of the 512-atom cluster with a Lorentzian broadening of  $2 \text{ cm}^{-1}$ . For alloys containing carbon, the supercell contains only a few C atoms and averages over 20–30 configurations were needed to obtain smooth spectra.

In order to obtain the optimal accuracy for phonons we have recalculated the Keating parameters to reproduce the optical phonon frequencies at the  $\Gamma$  and  $X$  points of the Brillouin zone. Also, we have included the scaling of  $\beta$  with the bond angle  $\theta$  to get the correct uniaxial deformation potentials. These parameters for Si, Ge, and SiGe are given in Table VI. Anharmonic scaling of the force constants was used as described above.

A typical calculated Raman spectrum is shown in Fig. 6 for a  $\text{Si}_{0.878}\text{Ge}_{0.11}\text{C}_{0.012}$  layer on Si(001). The calculation reproduces the characteristic peaks of the measured Raman spectrum.<sup>9</sup> By analyzing the atomic displacements for individual phonons the peaks can be assigned to Si-C, Si-Si, Si-Ge, and Ge-Ge modes as indicated in the figure.

#### B. Si-Si and Ge-Ge modes in $\text{Si}_{1-x}\text{Ge}_x$

Phonons of  $\text{Si}_{1-x}\text{Ge}_x$  alloys have been widely studied experimentally<sup>27–29</sup> and theoretically.<sup>30,11,31</sup> Here we focus on the dependence of the Si-Si and Ge-Ge Raman peaks on alloy composition and strain. The shift of the Raman peak positions in  $\text{Si}_{1-x}\text{Ge}_x$  alloys could be explained qualitatively as due to two effects.<sup>26</sup>

The first effect is that alloy disorder effectively confines the Raman-active phonon modes. Since the Ge atoms cannot follow the Si-Si vibrations and vice versa due to off resonance, the Si-Si modes are confined to the subspace of Si-Si bonds. In this picture, some Si atoms now have stationary (Ge) neighbors instead of Si atoms which

TABLE VI. Keating parameters  $\alpha$  and  $\beta$  in atomic units as fitted to the optical phonons of Si, Ge, and zinc-blende SiGe. The exponent  $\nu$  was fitted to the uniaxial phonon deformation potentials of Si and Ge.

	$\alpha$	$\beta$	$\nu$
Si	0.058	0.014	0.5
Ge	0.052	0.012	0.4
SiGe	0.055	0.013	

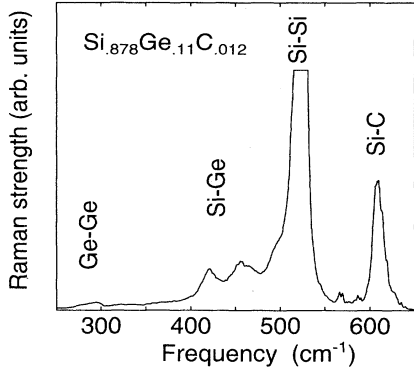


FIG. 6. Calculated first-order Raman spectrum of a random substitutional  $\text{Si}_{0.878}\text{Ge}_{0.11}\text{C}_{0.012}$  alloy layer on  $\text{Si}(001)$ .

oscillate with opposite phase as would be the case in pure Si, leading to a reduction of the restoring force and the phonon frequency. As a complementary interpretation, the site disorder in the alloy mixes optical phonons with a nonzero momentum (and consequently lower energy) into the Raman-active mode at  $\Gamma$ , again reducing the phonon frequency.

The second effect is that local strain shifts the phonon frequencies. The characteristic bond lengths in a semiconductor alloy, i.e., the Si-Si, Si-Ge, and Ge-Ge bonds in  $\text{Si}_{1-x}\text{Ge}_x$ , partially relax from their characteristic value in the ordered stoichiometric semiconductors towards an average bond length in the alloy.<sup>32,33,9</sup> This changes the bond stiffness as is described by Grüneisen's parameter. The shift of the Si-Si and Ge-Ge Raman peak positions in a free-standing layer relative to the positions in pure Si and Ge is thus the sum of two contributions which are due to mass disorder and microscopic strain:

$$\Delta\omega^{\text{fs}}(x) = \Delta\omega_{\text{mass}} + \Delta\omega_{\text{micro}} \quad (30)$$

An additional shift occurs when the alloy is macroscopically strained by external stress, for example if the layer is pseudomorphic to a substrate with a different lattice constant. The total Raman shift in this case is

$$\Delta\omega(x) = \Delta\omega^{\text{fs}}(x) + \Delta\omega_{\text{macro}}, \quad (31)$$

i.e., the sum of the shift for the corresponding free-standing alloy and a shift due to the macroscopic deformation.

The calculated shifts of the Raman peaks are summarized in Fig. 7 for the free-standing (fully relaxed)  $\text{Si}_{1-x}\text{Ge}_x$  alloys and for the biaxially strained layers when these are pseudomorphic to  $\text{Si}(001)$ . Available experimental data are also shown. Both the Si-Si and Ge-Ge frequencies show an almost linear dependence on the alloy composition with a maximal value in the pure materials. A substantially stronger dependence on the composition is found for the Si-Si mode. The macroscopic biaxial strain for pseudomorphic growth on  $\text{Si}(001)$  is seen

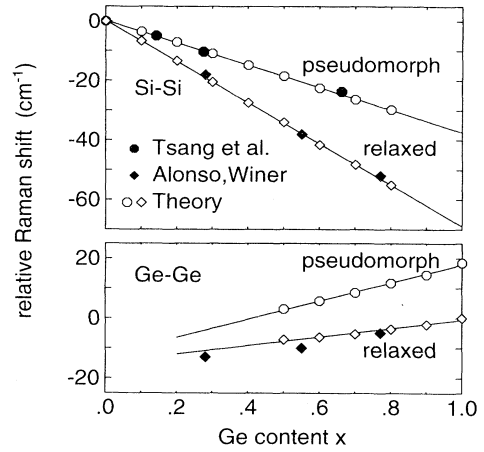


FIG. 7. Raman peak positions of Si-Si (upper part) and Ge-Ge modes (lower part) for free-standing (relaxed)  $\text{Si}_{1-x}\text{Ge}_x$  alloys and pseudomorphically strained layers on  $\text{Si}(001)$  in dependence on the Ge content  $x$ . All frequencies are given relative to the Si-Si and Ge-Ge frequencies in pure Si and Ge, respectively. Measured frequencies for a free-standing alloy taken from Alonso and Winer (Ref. 27) are shown as filled diamonds. Filled circles are experimental results for pseudomorphically strained layers due to Tsang *et al.* Ref. (29). Lines were fitted through the peak positions as calculated from the anharmonic Keating model (open symbols).

to harden both the Si-Si and the Ge-Ge modes. The experimental results are reproduced very well.

Using the Keating model, we can explicitly separate the Si-Si and Ge-Ge frequency shifts in free-standing alloys into the contributions due to mass disorder and to microscopic strain. In two auxiliary calculations, all bonds are taken to equal those of Si (respectively Ge) but the mass disorder is retained. The atoms then lie on the ideal lattice and are connected by equivalent bonds. Figure 8 shows that the mass disorder contribution  $\Delta\omega_{\text{mass}}$  softens the frequencies of the Si-Si as well as the Ge-Ge modes when the other atomic species is added. In a further numerical experiment, the mass of the Ge atoms was increased to infinity. This changes the phonon shifts by less than 5%, showing that the Ge atoms are essentially immobile in a Si-Si vibrational mode. Altogether, the suggested confinement effects are confirmed.

The effect of microscopic strain on the Raman frequencies is the difference of the full calculation (with microscopic and mass disorder) and the model calculation with mass disorder only. Both  $\Delta\omega_{\text{mass}}$  and  $\Delta\omega_{\text{micro}}$  depend almost linearly on the alloy composition  $x$  with the slopes given in Table VII. The strain contribution softens the Si-Si mode but hardens the Ge-Ge mode. As expected, the Si-Si bonds are slightly stretched in the alloy in proportion to the Ge content which reduces the bond stiffness. The compression of the Ge-Ge bonds in the alloy causes a hardening of Ge-Ge phonon mode with increasing Si content. In fact, for these modes the shift can be deduced to within 10% using the expression for the individual  $A$ - $B$  bond length as a function of the Ge

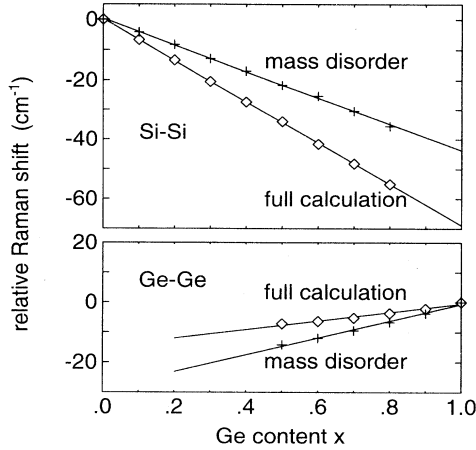


FIG. 8. Calculated relative shifts of Raman peak positions for  $\text{Si}_{1-x}\text{Ge}_x$  layers as in Fig. 7 (diamonds). Additional calculations were done for hypothetical systems in which all bonds are described by Si (respectively Ge) force constants and equilibrium bond length but with randomly distributed Si and Ge masses (crosses). Lines were drawn to guide the eye.

concentration<sup>9</sup> and the mode Grüneisen parameters of pure Si, respectively Ge. Overall, for the Ge-Ge mode the confinement and microscopic strain effects shift the frequency in opposite directions and partially compensate. For the Si-Si mode, both effects have the same sign, resulting in the observed stronger dependence on alloy composition.

Finally we discuss the additional shift due to the macroscopic biaxial strain when the layer is pseudomorphic to a substrate with different lattice constant. For a pure semiconductor, such effects are captured in the phonon deformation potentials. While we expect a linear relationship between the macroscopic strain and the phonon shift in the alloy, it is not clear whether the coefficient can be taken from the pure materials. For the case of (001) oriented interfaces considered here, the strain tensor is diagonal with the components

$$\epsilon_{xx} = \epsilon_{yy} = \epsilon, \quad \epsilon_{zz} = -\frac{2C_{12}}{C_{11}}\epsilon, \quad (32)$$

where  $\epsilon = (a_{\text{sub}} - a_{\text{lay}})/a_{\text{lay}}$  is given by the lattice mismatch between the substrate and the epilayer. Assuming Vegard's rule for the alloy lattice constant, a pseudomorphic  $\text{Si}_x\text{Ge}_{1-x}$  layer on Si (001) is biaxially strained

TABLE VII. Calculated relative shifts of Si-Si and Ge-Ge phonon modes in  $\text{Si}_{1-x}\text{Ge}_x$  as a function of the Ge content and substrate-imposed biaxial strain (see text).

	Si-Si	Ge-Ge
$\Delta\omega_{\text{mass}}$ ( $\text{cm}^{-1}$ )	$-44x$	$-28(1-x)$
$\Delta\omega_{\text{micro}}$ ( $\text{cm}^{-1}$ )	$-25x$	$14(1-x)$
$\Delta\omega_{\text{macro}}$ ( $\text{cm}^{-1}$ )	$-780\epsilon$	$-450\epsilon$

with  $\epsilon = -0.041x$ . In biaxially strained diamond or zinc-blende structure crystals the zone-center optical phonon splits into a singlet and a doublet state with frequencies given by<sup>34,19</sup>

$$\omega_d = \omega_0 - \gamma(2\epsilon_{xx} + \epsilon_{zz}) + \frac{p-q}{6\omega_0^2}(\epsilon_{xx} - \epsilon_{zz}), \quad (33)$$

$$\omega_s = \omega_0 - \gamma(2\epsilon_{xx} + \epsilon_{zz}) - \frac{p-q}{3\omega_0^2}(\epsilon_{xx} - \epsilon_{zz}). \quad (34)$$

Only mode  $\omega_s$  is observed in Raman backscattering  $z(x,y)\bar{z}$  geometry. Using the phonon deformation potentials of pure Si and Ge for the alloy Si-Si and Ge-Ge modes, we obtain  $\Delta\omega_{\text{macro}} = -790\epsilon \text{ cm}^{-1}$  and  $-460\epsilon \text{ cm}^{-1}$ , respectively. These estimates are in good agreement with the results of the full microscopic calculations (Table VII), showing that the macroscopic strain shift in the alloy can be obtained using the phonon deformation potentials of the pure materials.

Expressed in compact form, the calculated overall shift of the Si-Si peak when Ge is added and under biaxial strain is

$$\Delta\omega(x) = -69x - 780\epsilon \quad (\text{in cm}^{-1}), \quad (35)$$

where  $\epsilon = (a_{\text{sub}} - a_{\text{lay}})/a_{\text{lay}}$  is the substrate-imposed strain and  $x$  is the Ge content. This compares well with the experimental result<sup>27,29</sup>

$$\Delta\omega(x) = -68x - 830\epsilon \quad (\text{in cm}^{-1}), \quad (36)$$

as summarized in Ref. 35.

### C. Si-Si mode in alloys containing carbon

Basically in the same picture as discussed above, the change in the phonon spectrum when alloying with carbon can be analyzed in terms of strain shifts and confinement effects. The main difference to the SiGe system is in the magnitude of the two effects. Whereas a single C atom causes a large change in volume and consequently a large strain shift, the confinement effect per carbon and germanium atom is approximately the same. This is because neither the C nor the Ge atoms can participate in the Si-Si vibrations.

For a free-standing  $\text{Si}_{1-y}\text{C}_y$  alloy, the scaled Keating model predicts a shift of the Si-Si mode by  $\Delta\omega^{\text{fs}}(y) = y \times 210 \text{ cm}^{-1}$ , of which the confinement contribution is about  $-y \times 56 \text{ cm}^{-1}$ . For the case of Ge in Si, the corresponding coefficients were  $-69 \text{ cm}^{-1}$  and  $-44 \text{ cm}^{-1}$ , respectively. Thus, for carbon alloying the microscopic strain contribution is about ten times larger and essentially swamps out the confinement effect.

The effect of substrate-imposed biaxial strain can again be estimated using the phonon deformation potentials of pure Si. Despite the large local distortions in a random  $\text{Si}_{1-y}\text{C}_y$  alloy, the scaled Keating model shows that the average lattice constant  $a[\text{Si}_{1-y}\text{C}_y]$  is given to a good accuracy by Vegard's law

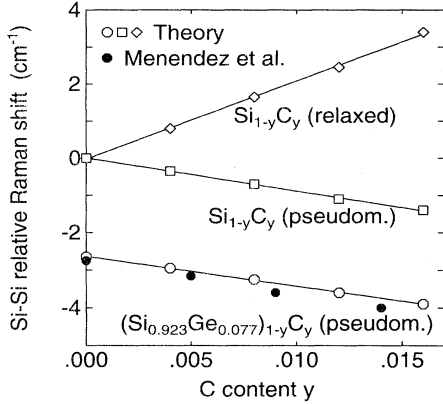


FIG. 9. Calculated relative shifts of the Si-Si Raman peak for relaxed  $\text{Si}_{1-y}\text{C}_y$  alloys (diamonds) and for pseudomorphic  $\text{Si}_{1-y}\text{C}_y$  (squares) and  $(\text{Si}_{0.923}\text{Ge}_{0.077})_{1-y}\text{C}_y$  (circles) layers on Si(001) in dependence on the C concentration  $y$ . Experimental results due to Menendez *et al.* (Ref. 35) for pseudomorphic  $(\text{Si}_{0.923}\text{Ge}_{0.077})_{1-y}\text{C}_y$  layers on Si(001) are included as filled circles.

$$a[\text{Si}_{1-y}\text{C}_y] = a[\text{Si}] - 2y(a[\text{Si}] - a[\text{SiC}]) \quad (37)$$

applied to a mixture of Si and  $\beta$ -SiC. From Eqs. (32) and (34) the shift is estimated to be  $\Delta\omega_{\text{macro}} = -315y \text{ cm}^{-1}$  for a carbon-containing layer pseudomorphic on Si (001). This agrees well with the result of the microscopic calculation  $\Delta\omega_{\text{macro}} = -300y \text{ cm}^{-1}$  shown in Fig. 9.

To conclude this section, we consider the case of a ternary  $\text{Si}_{1-x-y}\text{Ge}_x\text{C}_y$  alloy. One question of interest is whether the effects due to admixing of Ge and C atoms are additive, i.e., if there is a relation

$$\Delta\omega_{\text{SiGeC}}(x, y) = \Delta\omega_{\text{SiGe}}(x) + \Delta\omega_{\text{SiC}}(y) \quad (38)$$

Calculated frequencies of Si-Si Raman peaks for  $(\text{Si}_{0.923}\text{Ge}_{0.077})_{1-y}\text{C}_y$  layers on Si(001) are in quantitative agreement with measured peak positions of Menendez *et al.*<sup>35</sup> as shown in Fig. 9. Agreement is somewhat worse to another measurement<sup>9</sup> for the single stoichiometry  $\text{Si}_{0.878}\text{Ge}_{0.11}\text{C}_{0.012}$  which gave a shift of  $-6.5 \text{ cm}^{-1}$  relative to pure Si, as compared to the calculated value of  $-4.7 \text{ cm}^{-1}$ . As seen from Fig. 9, the addition of Ge to the  $\text{Si}_{1-y}\text{C}_y$  alloy evidently shifts the phonon peak by a value which is almost independent of the carbon concentration, namely by  $-2.7 \text{ cm}^{-1}$ . This agrees with the results of Sec. III B which predict a shift of  $-2.8 \text{ cm}^{-1}$  when going from pure Si to an alloy containing 7.7% germanium. Since the case considered here involves all three effects (microscopic and macroscopic strain as well as confinement), we conclude that all these terms are additive.

#### IV. SUMMARY

In this paper, the two-parameter Keating potential for the strain energy of diamond-structure crystals was generalized to include anharmonic effects. The aim was to

obtain a correct description of group-IV semiconductor alloys made from constituents with large differences in the atom sizes, primarily those containing carbon. *Ab initio* density-functional calculations were used to generate input data, which are difficult to obtain from experiment. The elastic properties of Si, C, Ge, and SiC were determined as a function of the crystal volume when this varies over a very large range. This information was used to obtain the Keating parameters  $\alpha$  and  $\beta$  as function of the volume. Interestingly, these were found to have the same behavior for all four studied semiconductors, namely to scale as the fourth and the seventh power, respectively, of the inverse nearest-neighbor distance. By taking this scaling as universal and including it in the (otherwise unchanged) Keating energy expression, we obtain a model which duplicates the standard model to second order in the atomic displacements but gives considerably different results when these displacements are large. Tests showed that the new model is much more successful in describing properties such as the elastic constants, phonon frequencies, or relaxed geometries when large distortions are involved.

The two-parameter Keating model, having only two fit parameters, cannot describe all features of the energy surface correctly at the same time. Thus, different sets of Keating parameters will generally be used, depending on whether the model was tuned for optimal description of the elastic constants or the phonon frequencies, or according to some other criterion. In effect, we have derived a simple procedure by which anyone can modify their favorite Keating model to make it applicable over a wider range of distortions.

This model was used to study the Raman-active optical phonon frequencies in disordered alloys containing Si, Ge, and C. Among other arguments, the standard Keating model obtains the wrong sign for the mode Grüneisen parameter in the pure materials and therefore the anharmonic model (which reproduces the experimental values) is appropriate here. The phonon frequencies for the alloy were determined by direct diagonalization of the dynamical matrix at the relaxed structure for supercells with 512 atoms, whereby the lattice sites were occupied randomly according to the stoichiometry. The results compare very well with available experimental data.

Based on previous discussions, the shifts of the phonon frequencies in the alloy are separated into three contributions: (i) confinement of the vibration to the sites of the relevant type, (ii) microscopic strain, i.e., the hardening or softening of the interatomic bonds as these change their length towards a common value, and (iii) a shift due to macroscopic biaxial strain if the layer is pseudomorphic to a substrate with a different lattice constant. An advantage of the calculation over experimental techniques is that these contributions can be quantified separately and then compared to predictions from simpler models. We find that the microscopic strain contribution can be described using the measured mode Grüneisen parameters for the pure materials together with the parameter which quantifies the degree of relaxation towards a common bond length in the alloy. Similarly, the effect of the macroscopic strain is well reproduced by using Veg-

ard's rule to estimate the lattice mismatch to the substrate and applying the measured deformation potentials in the pure materials to the ensuing strain.

In the context of the two strain contributions, the result of our simulation is to demonstrate that simple descriptions based on phonon deformation potentials for the pure materials can be used to describe the alloy. For the confinement effect, the calculations yield information which is not obviously available from experiment, namely the coefficients which quantify the shift of the different modes due to mass disorder.

*Note added in proof.* A previous paper<sup>36</sup> has followed the alternative path of directly fitting the numerous anharmonic force constants to a large database of theoretical and experimental values.

### APPENDIX

For convenience, we include expressions to calculate the forces within the anharmonic Keating model when the scaling with parameters  $m$ ,  $n$ , and  $\nu$  is used. Note that parameter  $\nu$  depends on the site because no universal scaling was found for it. The equilibrium bond length  $r_{ij}^0$  is here denoted by  $d_{ij}$ . Let  $i$  run over all sites of the lattice and let  $j$  run over the four neighbors of site  $i$ . For each such pair do the following:

$$\begin{aligned}\alpha_{ij} &= \alpha_{ij}^0 \left( \frac{r_{ij}^0}{r_{ij}} \right)^n, \\ E_{ij} &= \alpha_{ij} (r_{ij}^2 - d_{ij}^2)^2, \\ \mathbf{F}_{ij} &= \alpha_{ij} (r_{ij}^2 - d_{ij}^2) \left( 4 - n \frac{r_{ij}^2 - d_{ij}^2}{r_{ij}^2} \right) \mathbf{r}_{ij}.\end{aligned}$$

The contributions  $E_i$  and  $\mathbf{F}_{ij}$  are added to the total energy  $E$  and to the forces on the atoms  $\mathbf{F}_i$  as

$$\begin{aligned}E &\rightarrow E + E_{ij}, \\ \mathbf{F}_i &\rightarrow \mathbf{F}_i + \mathbf{F}_{ij}, \\ \mathbf{F}_j &\rightarrow \mathbf{F}_j - \mathbf{F}_{ij}.\end{aligned}$$

Still for the same pair  $(i, j)$ , let  $k$  also run over the neighbors of  $i$  in such a way that each pair  $(j, k)$  appears only once (that is,  $1 \leq j < k \leq 4$  if the neighbors are numbered from 1 to 4), let  $\theta$  be the bond angle, and evaluate the quantities

$$\begin{aligned}\beta_{ijk} &= \beta_{ijk}^0 \left( \frac{d_{ij}}{r_{ij}} \right)^m \left( \frac{d_{ik}}{r_{ik}} \right)^m \left( \frac{\theta_0}{\theta} \right)^{\nu_i}, \\ w &= \mathbf{r}_{ij} \cdot \mathbf{r}_{ik} - r_{ij}^0 r_{ik}^0, \\ E_{ijk} &= 2\beta_{ijk} w^2, \\ \mathbf{F}_j^{ijk} &= 2\beta_{ijk} w \left\{ 2\mathbf{r}_{ij} - \frac{mw}{r_{ik}^2} \mathbf{r}_{ik} \right. \\ &\quad \left. + \frac{\nu_i w}{\theta \sin \theta} \left[ \frac{\mathbf{r}_{ij}}{r_{ij} r_{ik}} - \frac{\mathbf{r}_{ik} \cos \theta}{r_{ik}^2} \right] \right\},\end{aligned}$$

as well as  $\mathbf{F}_k^{ijk}$  by exchanging  $j$  and  $k$  in the last equation. These values are added to the energy and the forces as

$$\begin{aligned}E &\rightarrow E + E_{ijk}, \\ \mathbf{F}_i &\rightarrow \mathbf{F}_i + \mathbf{F}_j^{ijk} + \mathbf{F}_k^{ijk}, \\ \mathbf{F}_j &\rightarrow \mathbf{F}_j - \mathbf{F}_j^{ijk}, \\ \mathbf{F}_k &\rightarrow \mathbf{F}_k - \mathbf{F}_k^{ijk},\end{aligned}$$

giving the total energy and forces when the loop over  $i$  is completed.

- 
- <sup>1</sup> P.N. Keating, Phys. Rev. **145**, 637 (1966).  
<sup>2</sup> K. Eberl and W. Wegscheider, in *Handbook of Semiconductors*, edited by S. Mahajam (Elsevier Science B.V., Amsterdam, 1994), Vol. 3A, p. 595.  
<sup>3</sup> S.C. Jain, *Germanium-Silicon Strained Layers and Heterostructures* (Academic Press, Boston, 1994).  
<sup>4</sup> S.S. Iyer, K. Eberl, M.S. Goorsky, F.K. LeGoues, J.C. Tsang, and F. Cardone, Appl. Phys. Lett. **60**, 356 (1992).  
<sup>5</sup> W. Wegscheider, J. Olajos, U. Menczigar, W. Dondl, and G. Abstreiter, J. Cryst. Growth **123**, 75 (1992).  
<sup>6</sup> S. de Gironcoli, P. Giannozzi, and S. Baroni, Phys. Rev. Lett. **66**, 2116 (1991).  
<sup>7</sup> J.G. Kirkwood, J. Chem. Phys. **7**, 506 (1939).  
<sup>8</sup> R. Tubino, L. Piseri, and G. Zerbi, J. Chem. Phys. **56**, 1022 (1972).  
<sup>9</sup> B. Dietrich, H. J. Osten, H. Rücker, M. Methfessel, and P. Zaumsiel, Phys. Rev. B **49**, 17185 (1994).  
<sup>10</sup> J.L. Martins and A. Zunger, Phys. Rev. Lett. **56**, 1400 (1986).  
<sup>11</sup> Z. Sui and I.P. Herman, Phys. Rev. B **48**, 17938 (1993).  
<sup>12</sup> W. Weber, Phys. Rev. B **15**, 4789 (1977).  
<sup>13</sup> M. Methfessel, C.O. Rodriguez, and O.K. Andersen, Phys. Rev. B **40**, 2009 (1989).  
<sup>14</sup> H.M. Polatoglou and M. Methfessel, Phys. Rev. B **41**, 5898 (1990).  
<sup>15</sup> W.R.L. Lambrecht, B. Segall, M. Methfessel, and M. van Schilfhaarde, Phys. Rev. B **44**, 3685 (1991).  
<sup>16</sup> N.E. Christensen and M. Methfessel, Phys. Rev. B **48**, 5797 (1993).  
<sup>17</sup> *Physics of Group IV Elements and III-V Compounds*, edited by K.-H. Hellwege and O. Madelung, Landolt-Börnstein, New Series, Group III, Vol 17, Pt. a (Springer-Verlag, Berlin, 1982).  
<sup>18</sup> D.L. Price, J.M. Rowe, and R.M. Nicklow, Phys. Rev. B **3**, 1268 (1971).  
<sup>19</sup> C.J. Buchenauer, M. Cardona, and F.H. Pollak, Phys. Rev. B **3**, 1243 (1971); F. Cerdeira, C.J. Buchenauer, F.H. Pollak, and M. Cardona, *ibid.* **5**, 580 (1972).  
<sup>20</sup> B.A. Weinstein and G.J. Piermarini, Phys. Rev. B **12**, 1172 (1975).  
<sup>21</sup> E. Anastassakis, A. Cantarero, and M. Cardona, Phys. Rev. B **41**, 7529 (1990).  
<sup>22</sup> W.A. Harrison, *Electronic Structure and the Properties of Solids* (Dover, New York, 1989).  
<sup>23</sup> P. Alinaghian, S.R. Nishitani, and D.G. Pettifor, Philos. Mag. B **69**, 889 (1994).  
<sup>24</sup> H. Rücker, M. Methfessel, E. Bugiel, and H.J. Osten, Phys.

- Rev. Lett. **72**, 3578 (1994).
- <sup>25</sup> S. de Gironcoli and S. Baroni, Phys. Rev. Lett. **69**, 1959 (1992).
- <sup>26</sup> J. Menendez, A. Pinczuk, J. Bevk, and J.P. Mannaerts, J. Vac. Sci. Technol. B **6**, 1306 (1988).
- <sup>27</sup> M.I. Alonso and K. Winer, Phys. Rev. B **39**, 10 056 (1989).
- <sup>28</sup> D.J. Lockwood and J.-M. Baribeau, Phys. Rev. B **45**, 8565 (1992).
- <sup>29</sup> J.C. Tsang, P.M. Mooney, F. Dacol, and J.O. Chu, J. Appl. Phys. **75**, 8098 (1994).
- <sup>30</sup> S. de Gironcoli, Phys. Rev. B **46**, 2412 (1992).
- <sup>31</sup> J. Zi, K. Zhang, and X. Xie, Phys. Rev. B **45**, 9447 (1992).
- <sup>32</sup> Y. Cai and M.F. Thorpe, Phys. Rev. B **46**, 15 872 (1992); **46**, 15 879 (1992); N. Mousseau and M.F. Thorpe, *ibid.* **46**, 15 887 (1992).
- <sup>33</sup> D.B. Aldrich, R.J. Nemanich, and D.E. Sayers, Phys. Rev. B **50**, 15 026 (1994).
- <sup>34</sup> E. Anastassakis, in *Light Scattering in Semiconductor Structures and Superlattices*, edited by D.J. Lockwood and J.F. Young (Plenum Press, New York, 1991), p. 173.
- <sup>35</sup> J. Menendez, P. Gopalan, G.S. Spencer, N. Cave, and J. Strane, Appl. Phys. Lett. **66**, 1160 (1995).
- <sup>36</sup> D. Vanderbilt, S.H. Taole, and S. Narasimhan, Phys. Rev. B **40**, 5657 (1989).

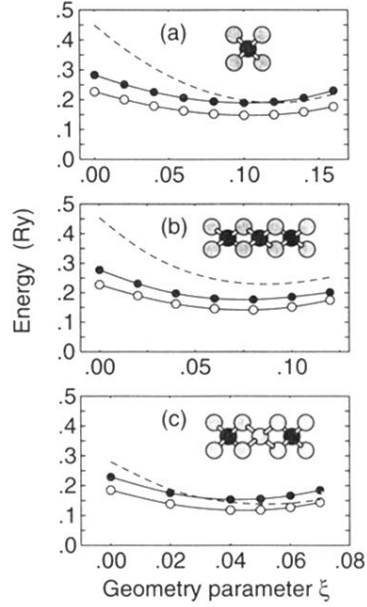


FIG. 5. Energy of formation for different arrangements of substitutional C atoms in a Si lattice: (a) single substitutional C impurity in a 32-atom supercell, (b) (001) monolayer of C atoms in a Si lattice, (c) half monolayer of a C atom arranged on a (001) plain in a  $(\sqrt{2} \times \sqrt{2})$  unit cell. The relaxation of the local geometry is always expressed by a single parameter  $\xi$  as specified in the main text. Insets indicate the nearest-neighbor environments of the C atoms (black) for the three cases. Results of *ab initio* calculations (full symbols) are differences between the total energy of the supercell and the total energies of the constituent atoms in the Si and  $\beta$ -SiC phases. All supercells contain one carbon atom. Open symbols are results of the anharmonic Keating model. Lines are indicated to guide the eye.